PROF. DR. G. KUPFER*
University of Bonn
53 Bonn, West Germany

Improvement of the Geometry of Aerial Photos

The more sophisticated models offered the smallest residuals, correcting for image deformation, uncorrected lens distortion and atmospheric refraction.

ABSTRACT: *Improvement in the size of the residual discrepancies in analytic aerotriangulation is obtained if sufficient attention is paid to the mathematical model and if regression analyses are applied. The different models studied indicate that the more sophisticated models offer the smallest residuals. The procedures are applied to data from the Rheidt test area. The analyses tend to correct for image deformation, uncorrected lens distortion and atmospheric refraction. The approach also applies variance-covariance and correlation coefficients.*

THE BASIC relationships between object space and image plane in photogrammetry are given by the equations of the central perspective. This holds true, with certain extensions, also for the more complex imaging systems, such as panorama cameras.

The relationships change significantly if the geometrical approach is replaced by a physical one. Nevertheless, a quite simple functional and stochastic model for the photogrammetric process is also used in analytical photogrammetry: image coordinates obtained by comparator measurements are treated stochastically as equally weighted and uncorrelated, and computational correlations are omitted as well. In general, the functional model will take photogrammetric refraction, average radial lens distortion determined in laboratory calibration and regular film deformation into account, sometimes also systematic comparator errors. Réseau photographs offer a further extension: irregular film deformation and the effects of lack of film flatness can also be corrected for. The first pragmatic attempt in the treatment of the geometry of aerial photographs was probably made in the 1950s at the British Ordnance Survey.[1]

The relationships of the analytical photogrammetric process are shown in Figure 1. All steps indicated in that figure should be described as well as possible by a stochastic and a functional model, because the process in its entirety is to be dealt with in photogrammetric practice. However, in following this approach, limits are set by a lack of knowledge about some of the steps and by economical considerations.

Most steps indicated in Figure 1 have already been investigated separately. A review of obtained results is given, e.g., in References 3. The figure also shows the steps that can be controlled by a réseau projected centrally and exposed simultaneously with the aerial photograph proper. In view of the contributions of film deformation and lack of film flatness to the overall photogrammetric errors, the use of a réseau camera will result in significant advantages. The application of réseau photography results in increased overall expenses. In addition, the réseau fails to give information about several important steps. This information can be obtained from photography taken over a test area. Although it might be less accurate than the determination of image deformation through the use of a réseau, this information still enables a comprehensive control of the entire relationship between object and measured image coordinates.

* Presented at the International Symposium on Image Deformation, Ottawa, Canada, June 1971.

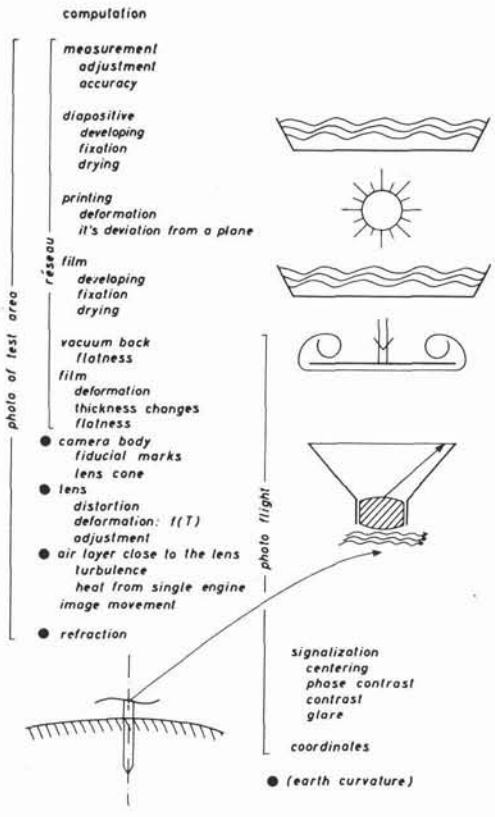

FIG. 1. The photogrammetric process in steps.

SYSTEMATIC falsification of the image geometry can be uncovered in single process steps if photographs are taken over a test area. Hence, such photographs enable partial calibration of the photogrammetric system. Values determined by laboratory calibration are introduced as approximate values. The results of such partial calibrations permit extensions to the functional model.

The stochastic model can also be improved by empirical determination of a variance-covariance matrix from the errors of the image coordinates derived from photography of test areas.

Practical tests have been performed using the almost-level Rheidt test area located in the vicinity of Bonn. The three coordinates of all the control points were determined by geodetic methods with *rms* errors of less than ± 10 mm. The distribution of the points is shown in Figure 2 where each point represents a group of three points placed in such a way that the distances between them vary from 1 m to 5 m. The area is approximately 2 km by 2 km.

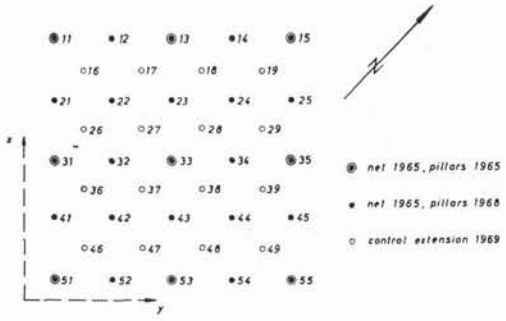

FIG. 2. The points of the test area.

ONE PHOTOGRAPH of the format 23 cm by 23 cm taken at a scale of approximately 1:11,000 covers the entire area, as do four photographs at a scale of approximately 1:5,500. Hence, the flight lines shown in Figure 3 were selected. For the various available camera types, the flying heights given in Table 1 should be used. So far, approximately 40 missions have been flown.

The image coordinates are derived by measuring glass diapositives twice, in most instances on Zeiss PSK stereo comparators. First, a spatial resection is computed for each photograph using nine points of the test area (control points) under the assumption that their geodetic coordinates are error free. More than 100 points then remain as check points if one photograph covers the whole test area.

TWO subroutines are mentioned explicitly: the correction of the image coordinates using fiducial marks and various polynomials, and the analysis of the errors in the check points after spatial resection.

The following transformations were used: Linear conformal transformation,

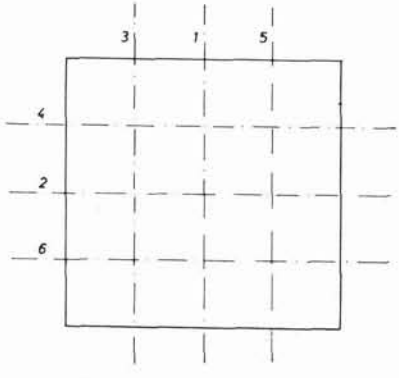

FIG. 3. Flight pattern for the test area for the scales 1:11,000 and 1:5,500.

TABLE 1. FLIGHT DATA FOR THE RHEIDT TEST FIELD

Type of Camera	Strip No.	Image Scale 1:	Flight Altitude Above	
			Ground (m)	Sea Level (m)
15/23	1,2	11,000	1,670	1,730
	3–6	5,500	840	890
8.5/23	1,2	11,000	930	990
	3–6	5,500	470	520
8.85/23	1,2	11,000	980	1,040
	3–6	5,500	490	550
21/23	1,2	11,000	2,310	2,370
	3–6	5,500	1,160	1,210
30/23	1,2	11,000	3,360	3,410
	3–6	5,500	1,680	1,730
11.5/18	1,2	14,000	1,610	1,660
	3–6	7,000	800	860
21/18	1,2	14,000	2,940	3,000
	3–6	7,000	1,470	1,530
10/14	1,2	18,000	1,800	1,860
	3–6	9,000	900	960
17/14	1,2	18,000	3,060	3,120
	3–6	9,000	1,530	1,590

$$x = a_0 + a_1x - a_2y'$$
$$y = a_3 + a_2x' + a_1y'. \quad (1)$$

Affine transformation,

$$x = a_{10} + a_{11}x' + a_{12}y$$
$$y = a_{20} + a_{21}x' + a_{22}y'. \quad (2)$$

Pseudo-affine transformation,

$$x = a_{10} + a_{11}x' + a_{12}x'y' + a_{13}y'$$
$$y = a_{20} + a_{21}x' + a_{22}x'y' + a_{23}y'. \quad (3)$$

Perspective transformation,

$$x = a_0 + a_1x' + a_2y' + a_4x'y' - a_3x'^2$$
$$y = a_5 + a_6x' + a_7y' - a_3x'y' + a_4y'^2. \quad (4)$$

Deformational transformation,

$$x = a_0 + a_1x' + a_2y' + a_4x'y' + a_3y'^2$$
$$y = a_5 + a_6x' + a_7y' + a_3x'y' + a_4x'^2. \quad (5)$$

Equations 2 and 4 lead in level terrain to identical results for the following spatial resection. The best results were obtained in spatial resection after performing the image deformation correction using Equations 5 which describe a circular image deformation. This deformation type was present in almost all films independent of the camera type used. The reduction of the residual errors on the check points amounted in extreme situations to more than 50 percent if the image deformation was corrected with Equations 5 instead of Equations 1.

The residual errors remaining after the spatial resections were projected onto the image plane and then investigated in view of regulations using third-order polynomials (see also Ziemann[8]):

$$dx = a_{10} + a_{11}x + a_{12}y + a_{13}xy + a_{14}x^2 + a_{15}y^2 + a_{16}x^2y + a_{17}xy^2 + a_{18}x^3 + a_{19}y^3 \quad (6)$$
$$dy = a_{20} + a_{21}x + \cdots$$

TORLEGARD[6] in Sweden used *optical polynomials* which correct primarily for radial and tangential distortion and hence, are restricted in their effectiveness within the overall system. Vlcek[7] selected orthogonal polynomials to express residual errors. He obviously did not, however, intend a partial system calibration. Finally, one might expect good results if the image coordinates are processed using Kraus' method[2]. This in spite of the fact that it does not fully correspond to the geometrical conception of the erroneous influences within the system that these influences should fade away according to the Gaussian curve, depending on the point distance.

The Polynomials 6 were determined for each flight mission from several photographs and then used to correct image coordinates obtained from this or a following flight using identical systems (camera magazine, film, airplane, etc.). Hence, they were used to eliminate systematic errors and were therefore called *regression* polynomials. This process was named *regression* procedure.

RESULTS for a few characteristic examples are given in Table 2 and Figures 4 to 6. All flights included in Table 2 were flown with cameras not equipped with a réseau. Values for the *adjacency accuracy* are given in column 5 of Table 2. These values are *rms* residual coordinate errors within the point groups, derived after bringing the centres of gravity determined photogrammetrically and geodetically into coincidence. As the points of the groups are, at an image scale of 1:11,000, located within 0.1 to 1.0 mm from each other, it can be assumed that the shift eliminated all systematic parts of the residual errors. The *adjacency accuracy* values for that scale, be-

TABLE 2. RESULTS OF SPATIAL RESECTIONS FOR SINGLE PHOTOGRAPHS

Flight Mission	*Type of Camera*	*Plane (Number of Engines)*	*Image Scale*	*RMS Error at Image Scale (μm)*				
				Within Point Nests	*Before Regression*		*After Regression*	
					σ_0	*Check Points*	σ_0	*Check Points*
1	2	3	4	5	6	7	8	9
5.65	Z 15/23 (1)	1	11,000	3.1	7.7	8.9	5.7	5.9
		1	5,500	3.6	8.8	10.7	5.2	6.8
6.65	Z 30/23	1	11,000	2.7	4.2	5.7	3.2	4.6
		1	5,500	3.7	5.2	7.2	4.9	7.1
8.65	W 15/23	2	11,000	2.9	4.3	5.1	2.7	4.3
		2	5,500	3.0	4.5	5.4	3.8	4.8
10.69	Z 15/23 (2)	1	11,000	3.4	7.0	7.2	4.8	5.9
		2	11,000	3.3	4.6	5.8	3.2	5.3

tween 2.7 μm and 3.4 μm, seem to indicate the limiting accuracy of photogrammetric methods.

Also given in Table 2 are the *rms* errors of unit weight σ_0 and the *rms* residual errors of the check-point coordinates determined by spatial resection for four flight missions prior to and after the regression procedure based on Equations 6 (columns 6 and 8 and columns 7 and 9 respectively). All values are average values each derived from several photographs. Comparison of columns 6 and 8 and of columns 7 and 9, respectively, demonstrates the effectiveness of the regression procedure in residuals. The effectiveness of this procedure is also demonstrated in Figures 4 to 6.

THE DEFORMATION of an example taken from flight mission 5.65 in Table 2 is displayed in Figure 4, where the solid lines indicate the residual deformation after a linear conformal transformation and the dashed lines indicate the residual deformation after a deformation procedure. The deformation of the photographs taken during this mission was larger than that of the photographs from the other missions. It is not possible to determine from the deformation, whether it was caused during the film handling in the aerial camera or during the film processing. Equation 5 proved to be significantly better in its reduction than Equation 1, both equations being based on only four fiducial marks located in the middles of the format sides.

The deformation of an example taken from flight mission 8.65 in Table 2 is shown in Figure 5, one example each from the two flight missions 10.69 in Figure 6. The latter two

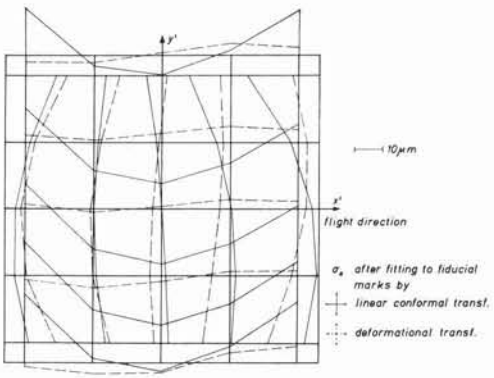

FIG. 4. Regression polynomials for flight mission 5.65.

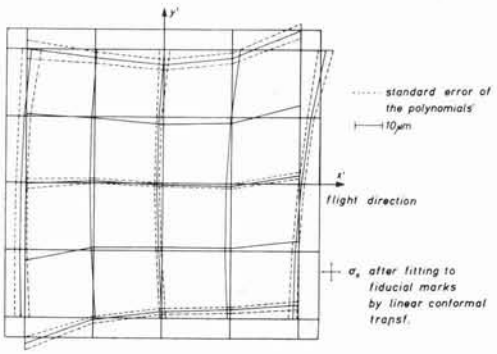

FIG. 5. Regression polynomials for flight mission 8.65.

flights were flown within an hour with systems identical with the exception of the airplane. The single-engine Dornier Do 27 airplane was replaced after the first flight by a twin-engine Dornier Do 28. The regression polynomials for both flights are practically identical (see Figure 6), although σ_0 is significantly different at the 95 percent confidence level (see Table 2).

Because of the similarity of the regular deformation, it must be concluded that the larger *rms* error of unit weight σ_0 for the first flight of that mission is a result of additional irregular distortions of approximately $\pm 4\,\mu m$ caused by the air in front of the camera lens using the single-engine airplane. Similar results were obtained in other missions. Even if the engine fumes are carefully diverted, it will for example not be possible to prevent the warm air leaving the oil cooler from moving towards the camera lens. This error source was found to produce errors of approximately the same size as the image deformation and it therefore contributes significantly in reducing the accuracy of analytical photogrammetric methods.

RESULTS FOR one of the missions flown with a normal-angle camera are also given in Table 2 (mission 6.65). A comparison of the values given in column 5 shows that the results (prior to the regression procedure) from that mission were better than the results obtained from wide-angle photography.

In the first three missions given in Table 2, photographs were taken not only at scale 1:11,000 but also at the scale 1:5,500. The residual errors derived from these latter photographs are generally larger than those from the smaller-scale photography, possibly as a result of inaccuracies in the determination of the geodetic coordinates, or also as a result of image motion. The results from the larger-scale photography were corrected using the regression Polynomials 6 derived from the smaller-scale photographs. It is obvious that this procedure yielded a good correction of regular deformations for the larger-scale, wide-angle photographs but failed to lead to any improvement for the larger-scale, normal-angle photographs. Because of the present lack of additional normal-angle photography results, it can only be assumed that the regression procedure leads to a significant reduction only if photographs are taken with cameras having a fairly large field angle.

THE PHOTOGRAPHS of the flight given last in Table 2 were used to derive empirically *a posteriori* correlation coefficients

$$r = \frac{\sum (dx_i dx_j + dy_i dy_j)}{\sum (dx_i dx_j + dy_i dy_i + dx_j dx_j + dy_j dy_j} \qquad (7)$$

with $i \neq j$ and the residual errors $dx_{i,j}$ and $dy_{i,j}$ of point pairs P_i, P_j of one or more photographs. These point pairs can be grouped according to their distances (Torlegard[6]; Kraus[2]). It is assumed that the correlation is strictly radially symmetrical. Some of the results are presented in Figure 7 by means of

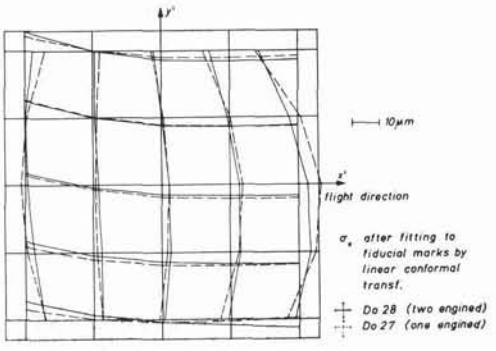

FIG. 6. Regression polynomials for flight mission 10.69.

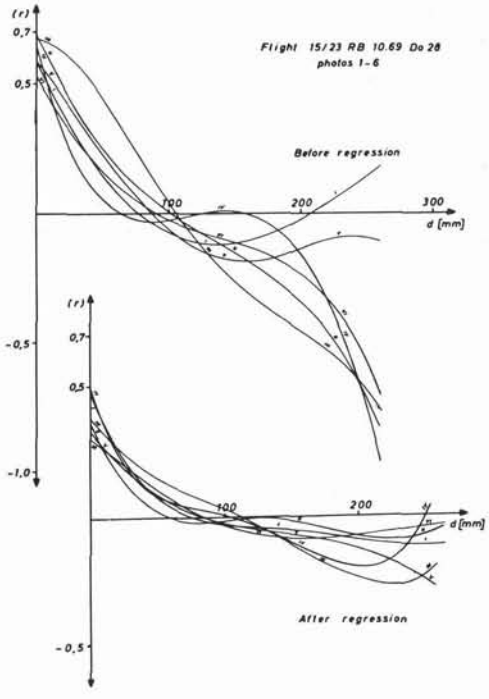

FIG. 7. Mission 10.69, correlation *a posteriori* ($r = f(s')$).

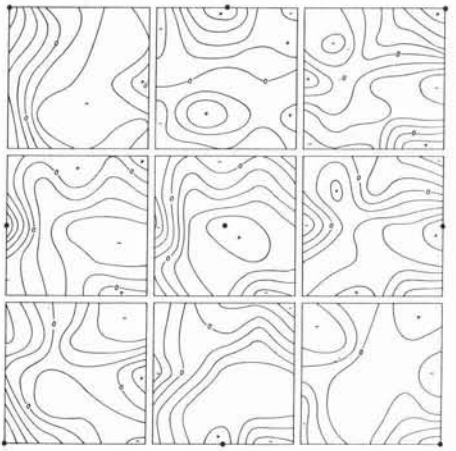

FIG. 8. Mission 10.69, correlation *a posteriori* ($r=f(x', y')$) *prior* to regression procedure. The interval between the isolines is $r=0.2$. Each square has the size of a photograph.

average curves. The values for r ranging between $+0.7$ and -1.0 prior to and from $+0.5$ and -0.3 after performing the regression procedure. The reduction and fairly good stabilization of the values for r for radial distances d over 80 mm is remarkable.

In addition, correlation coefficients r were also computed with respect to the image position. A certain point was chosen as a reference point and r was computed for all the other points. These computations were performed for all 12 photographs of that mission and averaged. Some of the results obtained are displayed in Figures 8 and 9 where curves connecting points with identical r are shown, in Figure 8 prior to and, in Figure 9, after performing the regression procedure. It is clear from these graphs that the correlation is neither radially symmetrical around the reference point nor clearly distance-dependent. A

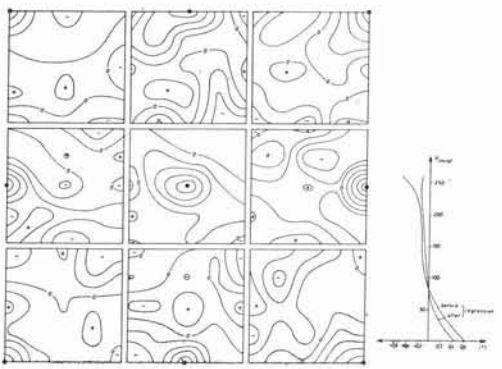

FIG. 9. Mission 10.69, correlation *a posteriori* ($r=f(x', y')$) *after* the regression procedure. For further explanation see caption to Figure 8.

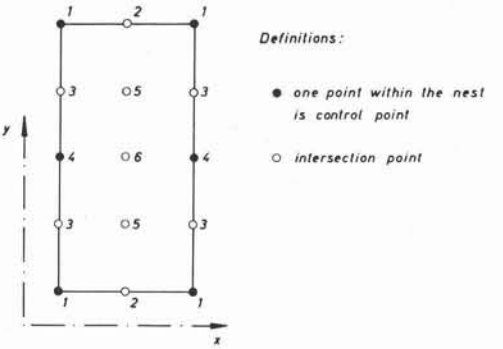

FIG. 10. Distribution of control and check points for spatial double-point resection using the 1:11,000 photographs.

refined stochastic model should consider this fact. However, the correlation coefficients are reduced sufficiently as a result of the regression procedure so that in this instance such an extension of the stochastic model does not seem to be desirable.

In spatial resections, algebraic correlations are small compared to physical correlations because of the use of a comparatively simple functional model[4].

THE method discussed suggests itself for application to the proper tasks of analytical photogrammetry, spatial double-point resection and aerotriangulation. An example for a model computation is given in Figure 10 and Table 3. The figure indicates the point distribution; the table shows residual errors in x, y position p and elevation h prior to and after performing of the regression procedure. Two examples for block computation using missions 5.65 and 8.65 are given in Figure 11 and Table 4.

In spite of the fact that the comparative material given here is not very extensive, it might be said that the applied regression pro-

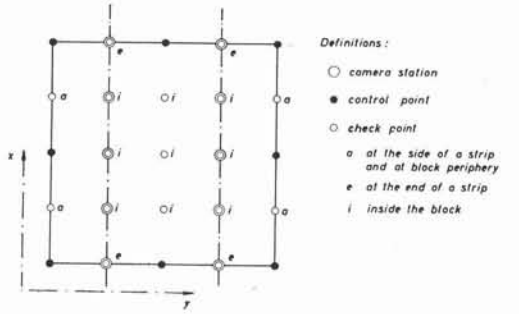

FIG. 11. Distribution of control and check points and camera stations for aerial triangulation using the 1:5,500 photography.

Table 3. Results of Spatial Resections for Pairs of Photographs

The values are average values of *rms* errors of the control points from two models formed from wide-angle photographs at 1:11,000. Image deformation correction with an affine transformation based on four fiducial marks.

RMS Error	*Number of Check Points*	*Before Regression*					*After Regression*				
		x	y	g	h	σ_0	x	y	g	h	σ_0
On the ground (mm)	39	34	43	54	100		31	38	48	98	
At image scale (μm)		3.0	3.8	4.9	0.0059%	4.1	2.8	3.4	4.4	0.0058%	3.2
Removed by regression (mm)									25	21	1.8
Improvement by regression (%)									11	2	22

Accuracy within nests of points:

	On the ground	In image scale
m_x	± 16 (mm)	± 1.5 (μm)
m_y	± 25	± 2.3
m_g	± 31	± 2.8
m_h	± 50	$\pm 0.0029\%\ h_g$

Table 4. Results of Aerial Triangulations (*rms* Errors of Check Points). Letters *i*, *e* and *a* Indicate Point Locations (See Figure 11).

Group of Check Points	*Number of Nests*	*Before Regression*					*After Regression*				
		x	y	p	h	σ_0	x	y	p	h	σ_0
Mission 5.65, "Deformational" transf., $c=152.50$; $M_b=1:5700$; $h_g=867$ m											
i (mm)	9	21	24	32	23		27	32	41	31	
e (mm)	4	21	30	38	81		16	34	38	71	
a (mm)	4	20	101	103	123		17	58	61	71	
On the ground (mm)	17	21	54	58	73		22	40	46	55	
In image scale (μm)		3.7	9.5	10.2	0.0084%	8.5	3.8	7.0	8.1	0.0064%	3.9
Removed by regression (mm)									35	48	
Removed by regression (μm)											7.6
Improvement by regression (%)									21	25	54
Mission 8.65, Linear conf. transf., $c=152.31$; $M_b=1:5700$; $h_g=862$ m											
i (mm)	9	15	14	21	30		16	13	21	25	
e (mm)	4	14	15	20	39		19	19	27	40	
a (mm)	4	18	51	54	41		12	20	23	25	
On the ground (mm)	17	16	28	32	35		16	17	23	29	
In image scale (μm)		2.8	4.9	5.6	0.0041%	5.4	2.8	3.0	4.0	0.0034%	3.3
Removed by regression (mm)									22	20	
Removed by regression (μm)											4.3
Improvement by regression (%)									28	17	39

cedure is as effective in improving model and block coordinates as it is in improving the results of single photograph spatial resections, particularly true as other flight missions gave similar results. Obviously the procedure fails to improve the elevations if single models are computed, but it yielded improvements for the elevation values within the blocks. The improvement of σ_0 as a result of regression applied to blocks is particularly outstanding and suggests that a significantly more homogeneous block is being obtained.

For the practical application of this method it is not necessary to have a large number of ground control points. The coefficients of the regressional polynomial can also be derived otherwise, e.g., if the same area is flown twice at two scales having ratios 1:2. Photographs at both scales are then used simultaneously to form blocks. This suggested method has been successfully tested over the test field using an iterative solution on nine control points only. A further reduction in the number of control points seems possible, so that a stage has been reached where an inclusion in each flight mission of the partial calibration by the regression procedure should be investigated.

ACKNOWLEDGEMENTS

The programs for model computation and block triangulation based on Dr. H. H. Schmid's formulation[5] were written by Drs. F. J. Heimes and Ö. Cenan. The PSK stereocomparator is on loan from the Deutsche Forschungsgemeinschaft. All computations were conducted on the IBM 7090/1410 of the Gesellschaft für Mathematik und Datenverarbeitung, Birlinghofen/Bonn, Germany. Dr. H. Ziemann kindly translated the German text.

REFERENCES

1. Arthur, D. W. G., "A stereocomparator technique for aerial triangulation." *Ordnance Survey Professional papers*, New Series No. 20, London 1955.
2. Kraus, K., "Correction of film deformation by least square interpolation." Presented in Ottawa, June 1971.
3. Kupfer, G., "Zur Geometrie des Luftbildes." German Geodetic Commission, Series C, No. 170, Munich 1971.
4. Morén, A., "The geometrical quality of aerial photographs." Ph.D. thesis, Stockholm 1967.
5. Schmid, H. H., "An analytical treatment of the orientation of a photogrammetric camera." *Photogrammetric Engineering*, XX, 1954, pp. 765–781.
6. Torlegard, K., "On the determination of interior orientation of close-up cameras under operational conditions using three-dimensional test objects." Ph.D. thesis, Stockholm 1967.
7. Vlcek, J., "Systematic errors of image coordinates. *Photogrammetric Engineering*, XXXV, 1969, pp. 585–593.
8. Ziemann, H., "Untersuchungen an Reseau-Aufnahmen." German Geodetic Commission, Series C, No. 104, Munich 1967.